7th International Conference on Debris-Flow Hazards Mitigation

How does particle-size segregation affect the fluidity of multi-granular debris flows?

Norifumi Hotta[a,*], Tomoyuki Iwata[b], Takuro Suzuki[c]

[a] *The University of Tokyo, Japan, 1-1-1 Yayoi, Bunkyo-ku, Tokyo 113-8657, Japan*
[b] *Chiba Prefectural Government Office, 1-1 Ichiba-cho, Chuo-ku, Chiba City, Chiba 260-8667, Japan*
[c] *Forestry and Forest Products Research Institute, 1 Matsunosato, Tsukuba, Ibaraki 305-8687, Japan*

Abstract

It is essential to consider the fluidity of a debris-flow front when calculating its impact. Here, we flume-tested monogranular and bigranular debris flows, and compared the results to those of numerical simulations. We used sand particles with diameters of 0.29 and 0.14 cm at two mixing ratios, of 50% and 50% (5:5), and 30% and 70% (3:7), respectively. Particle segregation was recorded using a high-speed video camera. We evaluated the fronts of debris flows at 0.5-s intervals. We then numerically simulated one-dimensional debris flows under the same conditions, and we used the mean particle diameter when simulating mixed-diameter flows. For monogranular debris flows, the experimental and simulated results were in good agreement in terms of flow depth, front velocity, and flux, but the bigranular debris flows were not well-simulated; the simulated flow depth was less than that found experimentally, and the front velocity and flux were greater. The differences may be attributable to the fact that the dominant shear stress was caused by the concentration of smaller sediment particles in the lower flow layers; such inverse gradations were detected in the debris flow bodies. In this situation, most shear stress is supported by smaller particles in the lower layers; the debris-flow characteristics become similar to those of monogranular flows. Consequently, the calculated front velocities were underestimated; particle segregation at the front of bigranular debris flows did not affect fluidity either initially or over time.

Keywords: Flume test; Multi-granular debris flow; Numerical simulation; Particle-size segregation

1. Introduction

Stony debris flows have been modeled by reference to internal stresses caused by interactions (such as collision and friction) between particles and the viscosity of pore fluid (Egashira et al., 1997; Takahashi, 2007). Numerical simulations have been used to reproduce and predict debris-flow behaviors (Nakagawa and Takahashi, 1997; Osti and Egashira, 2009). In both laboratory models and numerical simulations, a representative (uniform) particle size is usually assumed, although real-world debris flows include grains of many different sizes associated with inverse gradations and accumulation of large boulders at debris-flow fronts (Stock and Dietrich, 2006; Suwa et al., 2009).

Particle size greatly affects debris-flow fluidity; larger particles impart higher flow resistance (Takahashi, 2007). Hence, the fluidity of the debris-flow front, which is important in terms of impact forces, is affected by both particle size and particle admixing. Accumulation of boulders at the front causes the flow characteristics of that front to differ from those of the main body; these cannot be reflected in numerical simulations employing particles of uniform size.

Here, we flume-tested monogranular and bigranular debris flows and compared the results to those of numerical simulations, to determine the effects of particle segregation on the debris-flow front.

* Corresponding author e-mail address*: hotta.norifumi@fr.a.u-tokyo.ac.jp*

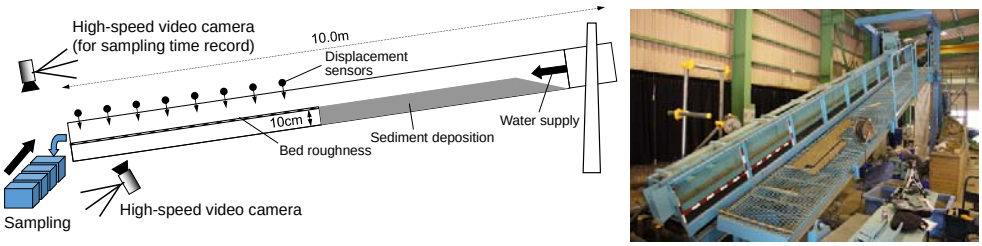

Fig. 1. The experimental setup.

2. Materials and Methods

2.1. Flume test

A channel of variable slope (10 m long and 10 cm wide) with a left-side glass sidewall was used for all experiments (Fig 1). The slope angle was set to 15°. The upper 3.5 m of the channel was filled with sand particles to a depth of 10 cm and connected to a lower stream 10 cm in height; this was a rigid bed 5 m in length to the surface, to which 2.9-mm-diameter sand particles were glued to impart roughness. To prevent overflow, the sand was watered to near-saturation immediately before each test. A steady flow of water (2,000 mL/s) was supplied from the upper end of the channel to generate debris flow by eroding the deposited sand.

Silica sands 0.29- and 0.14-cm in diameter were used; the mixing ratios were 50% and 50% (5:5), and 30% and 70% (3:7) (Table 1). Particle-size distribution affects the flow characteristics of debris flow in several ways. For example, fine sediment and its liquefaction change the fluidity (Nishiguchi et al., 2012; Hotta et al., 2013). In this study, we focused on particle segregation in stony debris flows. Sand particles of 0.29 and 0.14 cm were selected because they have been validated to behave as representative stony debris flows under this experimental setting (Hotta and Miyamoto, 2008; Hotta, 2012). Monogranular debris flows using each particle size, and bi-dispersed mixtures would simplify and clarify the particle segregation process.

Eight ultrasonic displacement sensors (E4C; Omron, Kyoto, Japan) were placed above the channel at 0.5-m intervals from 0.5–4.5 m distant to the downstream end; these monitored flow depth and timing. The temporal data were used to calculate front velocities. A high-speed video camera (EX-F1; Casio, Tokyo, Japan) was placed 0.5 m from the downstream end of the flow and recorded the debris flow from the side at 600 frames/s; we used the resulting images to evaluate the vertical velocity profiles and the locations of the larger (2.9 mm-diameter) particles by tracking the particles through the sequence of images. Five debris-flow samples from the front edges were collected at ca. 0.5 s intervals into a container with five separate rooms (Fig. 1), and one sample was also obtained from the main body at the lower end of the channel. We measured sediment concentrations and particle segregation.

Table 1. The silica sands used in the flume test.

Mixing ratio (0.29 *cm* : 0.14 *cm*)	Meam diameter (*cm*)
10 : 0	0.29
5 : 5	0.22
3 : 7	0.19
0 : 10	0.14

2.2. Numerical simulation

We performed a one-dimensional numerical simulation of debris flow. When modeling debris flows containing particles of two different diameters, we used the mean diameter (Table 1). The equations included a continuity equation for the debris flow, a continuity equation for the sediment, and a momentum equation:

$$\frac{\partial h}{\partial t}+\frac{\partial M}{\partial x}=E \tag{1}$$

$$\frac{\partial(\bar{c}h)}{\partial t}+\frac{\partial(c_t M)}{\partial x}=Ec_* \tag{2}$$

$$\frac{\partial M}{\partial t}+\beta\frac{\partial(uM)}{\partial x}=-gh\frac{\partial H}{\partial x}-\frac{\tau_0}{\rho_m} \tag{3}$$

where h is the flow depth, M is the discharge rate per unit width, E is the bed entrainment rate, $\bar{c}$ is the mean cross-sectional sediment concentration, c_t is the transported sediment concentration, c_* is the sediment concentration deposited in the channel, β is a compensation coefficient for momentum, u is the cross-sectional average velocity, g is the acceleration attributable to gravity, H is the elevation of the flow surface ($H = h + z_b$, where z_b is the bed elevation), τ_0 is the shear stress at the bed, and ρ_m is the density of debris flow. $\bar{c}$ and c_t are identical when assuming a uniform profile of sediment concentration. According to our measurements, c_* was 0.60. For τ_0, Itoh and Miyamoto (2002) developed constitutive equations, as follows:

$$\tau_0=\tau_{0y}+\rho f_b u^2 \tag{4}$$

$$\tau_{0y}=\left(\frac{\bar{c}}{c_*}\right)^{\frac{1}{5}}(\sigma-\rho)\bar{c}gh\cos\theta\tan\phi_s \tag{5}$$

$$f_b=\frac{25}{4}\left\{K_g+K_f\right\}\left(\frac{h}{d}\right)^{-2} \tag{6}$$

$$K_g=k_g\frac{\sigma}{\rho}(1-e^2)\bar{c}^{\frac{1}{3}} \tag{7}$$

$$K_f=k_f\frac{(1-\bar{c})^{\frac{5}{3}}}{\bar{c}^{\frac{2}{3}}} \tag{8}$$

where ρ is the density of water, σ is the density of the sediment particles (2.64), θ is the bed slope angle, ϕ_s is the internal friction angle of the sediment particles (34.0°), d *is* the mean diameter of the sediment particles, k_g is an experimental constant that was reported to be 0.0828 by Miyamoto (1985), according to Itoh et al. (1999) and, e, the coefficient of restitution of sediment particles, is equal to 0.85. k_f is a constant reflecting the interstitial space, which Egashira et al. (1988) evaluated as 0.16. Eqs (1)–(3) can be closed using an entrainment rate equation for E. We used the equation of Egashira et al. (1988):

$$\tan\theta_e=\frac{\bar{c}(\sigma/\rho-1)}{\bar{c}(\sigma/\rho-1)+1}\tan\phi_s \tag{9}$$

$$E=u\tan(\theta-\theta_e) \tag{10}$$

where θ_e is the equilibrium bed slope, which can be calculated based on a given sediment concentration (Takahashi,

1978).

3. Results

3.1. Flow depth and discharge

The experimental and simulated results were in close agreement in terms of the depths of monogranular, but not bigranular, debris flows (Fig 2). The experimental depths of bigranular flows were very similar to those predicted for monogranular flows of the smaller particles (diameter 0.14 cm) regardless of the mixing ratio (5:5 or 3:7 of 0.22- and 0.19-cm-diameter particles; Fig 2bc, respectively). Eqs (4) and (6) show that the flow depth differs by particle size, thus affecting flow resistance. However, the discharges did not differ greatly; the amounts of water supplied were identical. Eq (10), the entrainment rate equation, governing the sediment concentration is implicitly incorporating particle size (Hotta et al., 2015). Experimentally, the discharges of monogranular debris flows of 0.29- and 0.14-cm-diameter particles differed slightly, but calculations did not reveal any distinct difference (Fig 3a). The calculated and experimental data for the 0.14-cm-diameter-particle and mixed-particle debris-flow fronts disagreed (Fig 3b). The discharges were similar at particle mixing ratios of 5:5 and 3:7, as were the flow depths.

3.2. Velocity

The experimental and calculated monogranular debris-flow frontal velocities (both initially and over time) were in good agreement (Fig 4a). However, the experimental frontal velocity of bigranular debris flows were initially that of the 0.29-cm-diameter monogranular flow, and later became that of a debris flow containing particles of diameter equal to the mean of 0.14 and 0.29 cm, regardless of the mixing ratio (Fig 4bc). Fig 5 shows the experimental vertical distributions of particle velocities within bigranular debris flows. The velocities of the 0.14- and 0.29-cm-diameter particles did not differ at the same depth. The velocity profile indicated that the inclination was steeper in the flow body (7.9 and 6.9 s after the front had passed) than at the front (photos taken at 0.3 s; Fig 5a and 5b, respectively).

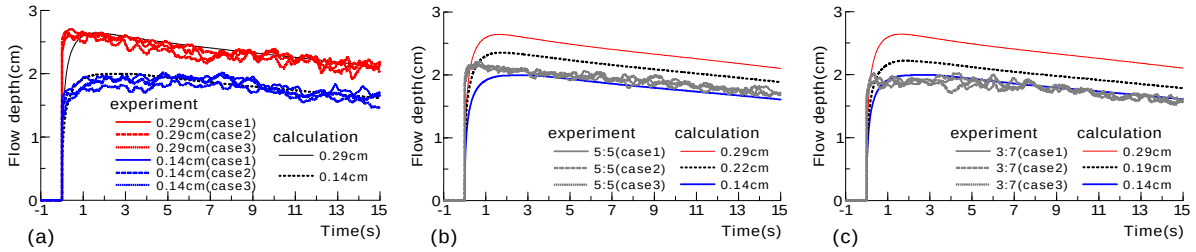

Fig. 2. Debris-flow depths over time of (a) monogranular flows, and (b) and (c), bigranular flows at particle mixing ratios (larger:smaller) of 5:5 and 3:7 respectively, at a point 0.5 m from the downstream end. The experimental flow depths are smoothed using a 0.4-s moving average.

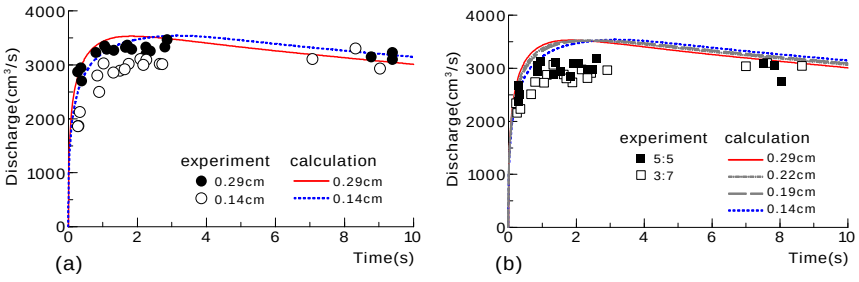

Fig. 3. Debris-flow discharge over time of (a) monogranular flows and (b) bigranular flows.

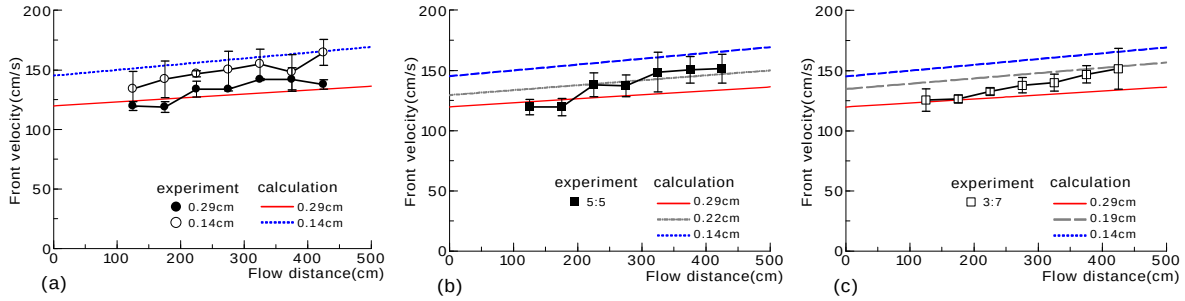

Fig. 4. Debris-flow frontal velocities over time of (a) monogranular flows, and (b) and (c), bigranular flows at particle mixing ratios (larger:smaller) of 5:5 and 3:7 respectively.

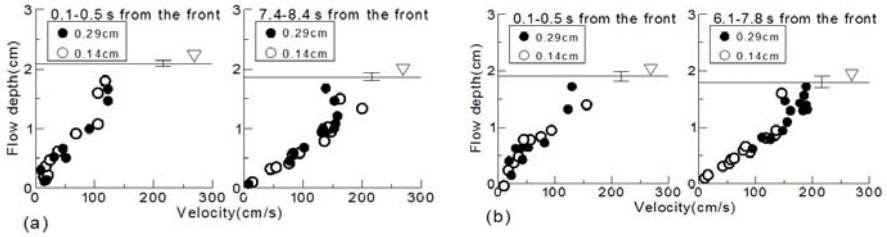

Fig. 5. Comparison between vertical velocity distributions of the front (left) and main body (right) of the debris flow at particle-mixing ratios (larger:smaller) of (a) 5:5 and (b) 3:7. The solid line indicates the average flow depth with error bar of the standard deviation.

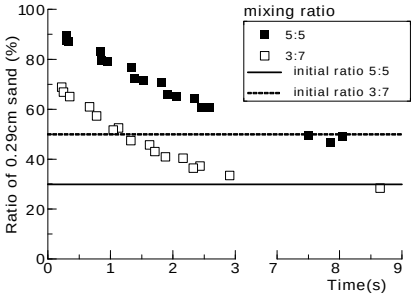

Fig. 6. The experimental particle mixing ratios of the fronts and main bodies of debris flows.

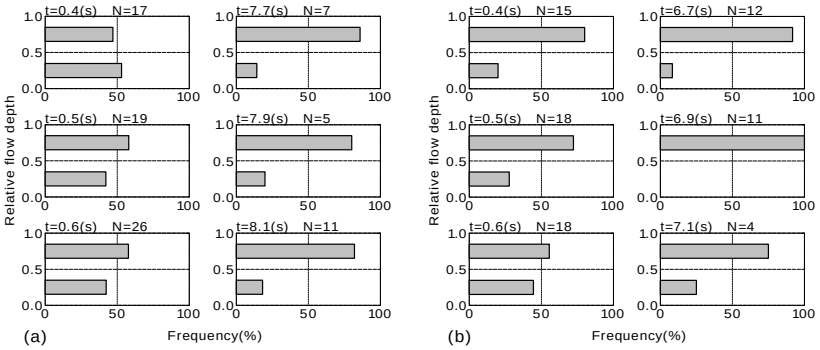

Fig. 7. Frequency distributions of 0.29 cm-diameter particles in the upper and lower layers of the experimental debris flows with particle mixing ratios (larger:smaller) of (a) 5:5 and (b) 3:7. N indicates the number of 0.29 cm-diameter particles in each image taken using the high-speed video camera. The relative flow depth was normalized by the surface level.

3.3. Particle segregation

Experimentally, the larger particles (0.29 cm) accumulated at the front (Fig 6). The extent of accumulation clearly differed by mixing ratio; the flow body retained the initial mixing ratio but inverse grading was apparent. Fig 7 compares large particle accumulation in the upper flow between the front and the main body. The extent of inverse grading was more significant in the main body; small particles thus predominated in the most inclined section of the velocity profile (Fig 5b).

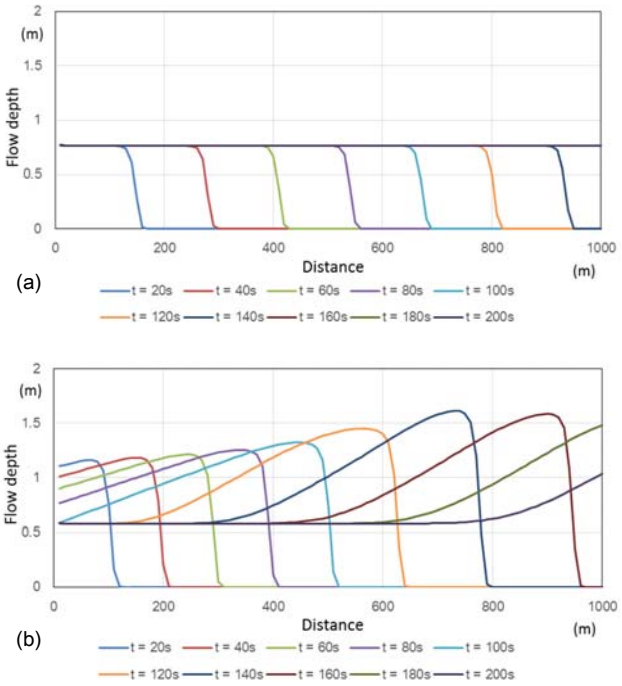

Fig. 8. Simulated profiles of the surges for (a) monogranular and (b) bigranular debris flows. In (b), the mean particle diameter was defined to decrease at the front of the body to simulate particle segregation.

4. Discussion and Conclusion

As shown in Figs 2 and 4, the behavior of bigranular debris flows could not be modeled using the mean particle diameter, whereas the behavior of monogranular flows could. This may be attributable to particle segregation; the uneven distribution of particles renders it inappropriate to use the mean particle diameter when seeking to model fluidity. Particle segregation is initially caused by inverse grading (Fig. 7), as shown in previous reports on bi-dispersed dry granular flow (Goujon et al., 2007) and saturated flow (Yamano and Daido, 1985). Thus, small particles concentrate in the lower layer, characterized by a steeper velocity profile (Fig 5b), suggesting that most shear stress is borne by small particles. This is consistent with the fact that the behavior of bi-granular flows corresponds to that predicted for flows with small particles only, regardless of the mixing ratio, after the flow has developed sufficiently (Fig 2bc). Similar behavior was pointed out by Linares-Guerrero et al. (2007) through numerical simulation, who used the discrete element method to model bi-dispersed dry granular flow.

On the other hand, at the start of the debris flow, when differently sized particles had not yet segregated, the fluidity of bigranular flows was similar to that of a monogranular flow of 2.9-cm-diameter particles (Fig 4bc). Large dispersed particles within the flow body may dominate the internal stress environment, but, as the flow descended, the flow velocity changed to that of a flow of smaller-sized particles (Fig 4bc). Thus, in reality, debris-flow motion, especially that of the front, is not adequately described by numerical simulations featuring a uniformly sized particle.

In a further example, we compare the simulated profiles of the surges for monogranular and bigranular debris flows in Fig 8. The calculation employs the same model as used in Section 2.2 but was applied at a real scale so that we

could clarify the different performances after simulating the distances descended by mono- and bigranular debris flows. In Fig 8b, the frontal accumulation of large boulders is modeled by gradually decreasing the particle size; the larger particles accumulate at the front and the smaller ones accumulate in the main body, and the average particle size is that of a monogranular debris flow (Fig 8a). The monogranular flow exhibits steady motion; the velocity of the mixed-particle flow is lower, in contrast to the observed results (Fig. 4). The flow depth of the bigranular flow increases as the main body catches up to the front, due to the greater velocity of the main body, which consists of smaller particles. This result conflicts with that of the experiment (Fig. 2). Thus, the results of the calculations based on a basic particle-segregation model that simply incorporates the transition of the mean particle size differ markedly from our experimental results.

Particle segregation in a debris flow is not simple. Debris flow fluidity may be controlled by local conditions, such as the vertical distribution of particle sizes, resulting in an uneven structure of internal stresses. Further understanding of particle segregation is needed for better assessment of on-site debris flows that contain a variety of particle sizes.

References

Egashira, S., Ashida, K., and Sasaki, H., 1988, Mechanics of debris flow in open channel, *in* Proceedings, Japanese Conference on Hydraulics, Japan Society of Civil Engineers, v. 32, p. 485–490. (in Japanese with English summary)

Egashira, S., Miyamoto, K., and Itoh, T., 1997, Constitutive equations of debris flow and their applicability, *in* Proceedings, International Conference on Debris-Flow Hazards Mitigation, 1st, San Francisco, p. 340–349.

Goujon, C., Dalloz-Dubrujeaud, B., and Thomas, N., 2007, Bidisperse granular avalanches on inclined planes: A rich variety of behaviors: The European Physical Journal E 23, p. 199–215, doi:10.1140/epje/i2006-10175-0.

Hotta, N., and Miyamoto, K., 2008, Phase classification of laboratory debris flows over a rigid bed based on the relative flow depth and friction coefficients: International Journal of Erosion Control Engineering, v. 1, p. 54–61, doi:10.13101/ijece.1.54.

Hotta, N., 2012, Basal interstitial water pressure in laboratory debris flows over a rigid bed in an open channel: Natural Hazards and Earth System Sciences, v, 12, p. 2499–2505, doi:10.5194/nhess-12-2499-2012.

Hotta, N., Kaneko, T., Iwata, T., and Nishimoto H., 2013, Influence of fine sediment on the fluidity of debris flows: Journal of Mountain Science, v. 10, p. 233–238, doi:10.1007/s11629-013-2522-y.

Hotta, N., Tsunetaka, H., and Suzuki, T., 2015, Interaction between topographic conditions and entrainment rate in numerical simulations of debris flow: Journal of Mountain Science, v. 12, p. 1383–1394, doi:10.1007/s11629-014-3352-2.

Itoh, T., Miyamoto, K., 2002, Study on one dimensional numerical simulation of debris flow, *in* Proceedings, Japanese Conference on Hydraulics, Japan Society of Civil Engineers, v. 46, p. 671–676. (in Japanese with English summary)

Itoh, T., Egashira, S., Miyamoto, K., Takeuchi, T., 1999, Transition of debris flows over rigid beds to over erodible beds, *in* Proceedings, Japanese Conference on Hydraulics, Japan Society of Civil Engineers, v. 43, p. 635–640. (in Japanese with English summary)

Linares-Guerrero, E., Goujon, C., and Zenit, R., 2007, Increased mobility of bidisperse granular avalanches: Journal of Fluid Mechanics, v. 593, p. 475–504, doi:10.1017/S0022112007008932.

Mymaoto, K., 1985, Study on the grain flows in Newtonian fluid [Ph.D. thesis]: Ritsumeikan University, 155 p. (in Japanese)

Nakagawa, H., and Takahashi, T., 1997, Estimation of a debris flow hydrograph and hazard area, *in* Proceedings, International Conference on Debris-Flow Hazards Mitigation, 1st, San Francisco, p 64–73.

Nishiguchi, Y., Uchida, T., Takezawa, N., Ishizuka, T., and Mizuyama, T., 2012, Runout characteristics and grain size distribution of large-scale debris flows triggered by deep catastrophic landslides: International Journal of Erosion Control Engineering, v. 5, p. 16–26, doi: 10.13101/ijece.5.16.

Osti, R., and Egashira, S., 2008, Method to improve the mitigative effectiveness of a series of check dams against debris flows: Hydrological Processes, v. 22, p. 4986–4996, doi: 10.1002/hyp.7118.

Stock, J. D., and Dietrich, W. E., 2006, Erosion of steepland valleys by debris flows: Geological Society of America Bulletin, v. 118, p. 1125–1148, doi:10.1130/B25902.1.

Suwa, H., Okano, K., and Kanno, T., 2009, Behavior of debris flows monitored on test slopes of Kamikamihorizawa Creek, Mount Yakedake, Japan: International Journal of Erosion Control Engineering, v. 2, p. 33–45, doi:10.13101/ijece.2.33.

Takahashi, T., 1978, Mechanical characteristics of debris flow: Journal of Hydraulic Division, American Society of Civil Engineering, v. 104, p. 1153–1169.

Takashi, T., 2007, Debris Flow: Mechanics, Prediction and Countermeasures: Taylor and Francis, Balkema, 448 p.

Yamano, K., and Daido, A., 1985, The mechanism of granular flow of mixed diameter composed two diameters: Journal of Japan Society of Civil Engineers, v. 357, p. 25–34. (in Japanese with English summary)